Predicting Daily Insolation with Hourly Cloud Height and Coverage[1]

T. P. MEYERS AND R. F. DALE

Agronomy Department, Purdue University, West Lafayette, IN 47907

(Manuscript received 28 November 1982, in final form 7 February 1983)

ABSTRACT

Solar radiation information is used in crop growth, boundary layer, entomological and plant pathological models, and in determining the potential use of active and passive solar energy systems. Yet solar radiation is among the least measured meteorological variables.

A semi-physical model based on standard meteorological data was developed to estimate solar radiation received at the earth's surface. The radiation model includes the effects of Rayleigh scattering, absorption by water vapor and permanent gases, and absorption and scattering by aerosols and clouds. Cloud attenuation is accounted for by assigning transmission coefficients based on cloud height and amount. The cloud transmission coefficients for various heights and coverages were derived empirically from hourly observations of solar radiation in conjunction with corresponding cloud observations at West Lafayette, Indiana. The model was tested with independent data from West Lafayette and Indianapolis, Madison, WI, Omaha, NE, Columbia, MO, Nashville, TN, Seattle, WA, Los Angeles, CA, Phoenix, AZ, Lake Charles, LA, Miami, FL, and Sterling, VA. For each of these locations a 16% random sample of days was drawn within each of the 12 months in a year for testing the model. Excellent agreement between predicted and observed radiation values was obtained for all stations tested. Mean absolute errors ranged from 1.05 to 1.80 MJ m^{-2} day^{-1} and root-mean-square errors ranged from 1.31 to 2.32 MJ m^{-2} day^{-1}. The model's performance judged by relative error was found to be independent of season and cloud amount for all locations tested.

1. Introduction

Solar radiation information is used in crop growth, boundary layer, entomological and plant pathological models, and in determining the potential use of active and passive solar energy systems. For many applications of solar radiation information, an accurate assessment of the spatial distribution of daily insolation is required. Since the existing network density of solar radiation stations is not adequate to provide this desired distribution, solar radiation models can be employed to supplement the solar radiation measurements with estimates made from observations of cloud amounts and heights available from the denser network of aviation weather reporting stations.

Recently, satellite brightness measurements from the Geostationary Operational Environmental Satellite (GOES) have been shown to be effective in estimating daily insolation at the surface (Brakke and Kanemasu, 1981; Gautier *et al.*, 1980). Estimates of daily insolation within 10% of the mean (Gautier *et al.*, 1980) were achieved at the expense of manipulating extremely large GOES data sets for high spatial and temporal resolution. Solar radiation models using the reported hourly cloud type and coverage have been shown to estimate daily insolation generally to within 15–20% of the observed values (Davies *et al.*, 1975; Suckling and Hay, 1977; Atwater and Ball, 1981). A limitation with these models arises from the fact that observations of cloud type and coverage are generally not reported hourly. Similarly, although Meyers *et al.* (1982) found opaque cloudiness highly correlated with daily insolation, observations of opaque cloudiness are not transmitted and can only be obtained from the observational forms from first- and second-order stations.

Data which are regularly reported for aviation purposes on an hourly basis are cloud base height and coverage. The objective in this paper is to use this information to estimate daily insolation.

2. Methodology

In the absence of clouds, solar radiation (SR) passing through the atmosphere is attenuated by Rayleigh scattering, absorption by water vapor and permanent gases, and aerosol scattering and absorption. Attenuation by each of these components is strongly dependent on wavelength and the optical air mass. Rayleigh scattering is strongest in the blue region of the solar spectrum. Water vapor absorption takes place primarily in the near infrared (IR) bands. Aerosol scattering and absorption are complex functions of the radius of the scattering particle, the scattering angle, the particle concentration and wavelength. For

[1] Journal Paper No. 9274, Purdue University Agricultural Experiment Station. Partially supported by NSF Atmospheric Sciences Section Grant ATM 8021075.

clear skies, a general expression used to compute irradiance at the surface is

$$I = I_0(\cos Z)T_R T_g T_w T_a, \quad (1)$$

where I_0 is the extraterrestrial flux density at the top of the atmosphere on a surface normal to the incident radiation, Z the solar zenith angle, and T_i the transmission coefficients after Rayleigh scattering (R), absorption by permanent gases (g) and water vapor (w), and absorption and scattering by aerosols (a). Eq. (1) is valid for monochromatic radiation, but it has been used for broad-band models to approximate the real atmosphere (Atwater and Ball, 1981).

As a result of changes in the earth–sun distance through the year, the impinging radiation at the top of the atmosphere changes by the following relation:

$$I_0 = 1353 \text{ W m}^{-2}\{1 + 0.034 \times \cos[2\pi(n - 1)/365]\}, \quad (2)$$

where n is the Julian day. The solar zenith angle is computed from

$$Z = \cos^{-1}(\sin\gamma \sin\delta + \cos\gamma \cos\delta \cos H), \quad (3)$$

where γ is the latitude, δ the declination angle, and H the hour angle. A subroutine by Walraven (1978) which defines δ and H accurately was used to compute Z to the nearest 0.10°. An empirical relationship for the attenuation by Rayleigh scattering and permanent gas absorption was given by Kondratyev (1969). This expression was later modified by Atwater and Brown (1974) to include the radiation scattered in the forward direction. The formula is

$$T_R T_g = 1.021 - 0.084 \times [m(949p \times 10^{-5} + 0.051)]^{1/2}, \quad (4)$$

where p is the surface pressure (Kpa), and m is the optical air mass at a pressure of 101.3 kPa given by

$$m = 35(1224 \cos^2 Z + 1)^{-1/2}. \quad (5)$$

An expression by McDonald (1960) was used to compute the broad-band transmission after water vapor absorption. This expression is

$$T_w = 1 - 0.077(um)^{0.3}, \quad (6)$$

where u is the precipitable water vapor. As the radiosonde network is sparse, the precipitable water was estimated from the surface dewpoint with an expression by Smith (1966), i.e.,

$$u = \exp[0.1133 - \ln(\lambda + 1) + 0.0393T_d], \quad (7)$$

where T_d is the daily average dewpoint (°F) and λ a constant derived empirically for latitude and season. This approximation is justified by the high correlations found between T_d and precipitable water vapor (Reitan, 1963; Bolsenga, 1965). Values of λ were taken from Smith (1966, Table 1).

Aerosol attenuation is complex and requires numerous input parameters, most of which are not available from standard meteorological observations. Therefore a simple treatment, using an expression by Houghton (1954) of the form,

$$T_a = x^m, \quad (8)$$

was used. In this expression, m again is the optical air mass and x a constant derived empirically as a residual in (1) for clear sky conditions. When solving for x, errors in parameterizing Rayleigh scattering, and absorption by water vapor and permanent gases are included in the residual. The residual x, however, was found to be almost constant. A value of 0.935 was derived for all stations except Miami and Lake Charles, where the estimated x value was 0.95.

To check the empirical equations for T_R, T_g, T_w and T_a, SR was estimated for randomly selected clear days in 1980 for the National Weather Service (NWS) stations at Seattle, WA, Indianapolis IN, Nashville, TN, Madison, WI, Omaha, NE, Columbia, MO, Sterling, VA, Miami, FL, Lake Charles, LA, Phoenix, AZ, and Los Angeles, CA. The year 1976 was used for West Lafayette, where the solar radiation measurements were made at the cooperative NWS-Purdue University Agronomy Farm and the cloud observations at the Federal Aviation Administration (FAA) Flight Service Office at Purdue Airport, 6 km southeast of the Agronomy Farm. Solar radiation was computed every 6 min and summed from sunrise to sunset to obtain the daily values. The predicted values were then plotted against the observed values.

The situation becomes more complex when clouds are introduced. In other models, cloud effects are simulated by including cloud transmission coefficients based on cloud type. Following a method by Manabe and Strickler (1964), the transmission T_c after cloud attenuation is given as

$$T_c = \prod_{i=1}^{n_c} [1 - c_i(1 - t_i)], \quad (9)$$

where n_c is the number of cloud layers, c_i the coverage of the ith layer, and t_i the transmission coefficient for the cloud type. Eq. (9) was originally developed for large horizontal areas rather than a single point, as in the case of a pyranometer. It was assumed that the reported cloud coverage between the pyranometer and the sun averaged over time gave an *effective* cloud cover and cloud transmission. Davis *et al.* (1979) found that with fractional cloud coverage, the transmission was zenith-angle dependent because of the vertical extent of finite clouds. Since the reported cloud information does not include the vertical cloud dimension, however, this finite cloud effect was not defined. The cloud transmission coefficients frequently used in models are those by Haurwitz (1948), who measured the transmissivities for eight of the ten

cloud genera. Hourly observations of cloud type and amount can be utilized to compute hourly totals of insolation, which are then summed to obtain the daily SR. This scheme works reasonably well, providing hourly observations of cloud type and amount are available (Atwater and Ball, 1978). However, cloud type and amount are only reported at 3 h intervals, mostly from first-order stations.

The hourly aviation report, also recorded on form MFI-10C, includes the cloud base height and amount categories at each of several levels. To utilize this form of cloud information, transmission coefficients were computed for various cloud base heights and coverages. This was done empirically by including the T_c component [(9)] in Eq. (1) and solving the equation for t_i for hours in which only a single cloud layer was observed. When solving for the cloud transmission t_i, the portion of the radiation reflected from the surface to the cloud base and then back to the earth's surface must also be considered. This component is a minor contribution in the summer, when the albedo of green vegetation is usually on the order of 20%. In the winter, however, the cloud return reflectance of the high albedo from a fresh snow cover can be responsible for 35–40% of the incoming SR on cloudy days. Any secondary reflection between clouds was neglected to simplify the computations.

Including the contribution from ground to cloud to ground reflectance with the effects of clouds as given by (9), Eq. (1) becomes

$$I = I_0 \cos Z T_R T_g T_w T_a \prod_{i=1}^{n_c} [1 - c_i(1 - t_i)] \times (1 - r_e r_c)^{-1}, \quad (10)$$

where r_e is the surface albedo and r_c the cloud albedo. The earth's surface albedo (r_e) in the vicinity of the SR measurements was assumed to be 0.2 and with snowcover, 0.65. The cloud albedo (r_c) was assumed to be 0.5 for all clouds with bases less than 5486 m (18 000 ft) and 0.0 for those greater than 5486 m. Solving Eq. (10) for a single cloud layer, the effective cloud transmission becomes

$$t_i = I(1 - r_e r_c)(I_0 \cos Z T_R T_g T_w T_a c_i)^{-1} + (c_i - 1)c_i^{-1}. \quad (11)$$

Using hourly values of SR from the Purdue Agronomy Farm from 1970–75 with corresponding cloud base height and amount information from the Purdue Airport, t_i [Eq. (11)] populations were generated for various cloud base heights and coverages. The generated populations of cloud transmission coefficients were grouped according to cloud base height and coverage. The cloud height classifications were

1) <1219 m (4000 ft)
2) 1219–3048 m (4000–10 000 ft)
3) 3048–5486 m (10 000–18 000 ft)
4) >5486 m (18 000 ft)
5) >5486 m (18 000 ft) thin.

Each of the five groups were partitioned into overcast (OVC) and broken (BKN) cloud layers because preliminary analysis showed considerable differences in transmissivities between OVC and BKN clouds for all layers. Values of c_i were determined from preliminary analysis. For OVC coverage, c_i was set equal to 1.0, for BKN 0.7, and for scattered (SCT) 0.3. The hourly observations of SR and cloud base heights were selected between 1100 and 1400 LT, when the sun is at its zenith, to minimize observational errors resulting from the clouds not being in the direction of the sun. Histograms of t_i were constructed for each category of cloud height and coverage. Most of the distributions were skewed, with two examples (low overcast and high thin broken) shown in Fig. 1. Because of this skewness and because preliminary testing showed better results when t_i medians were used,

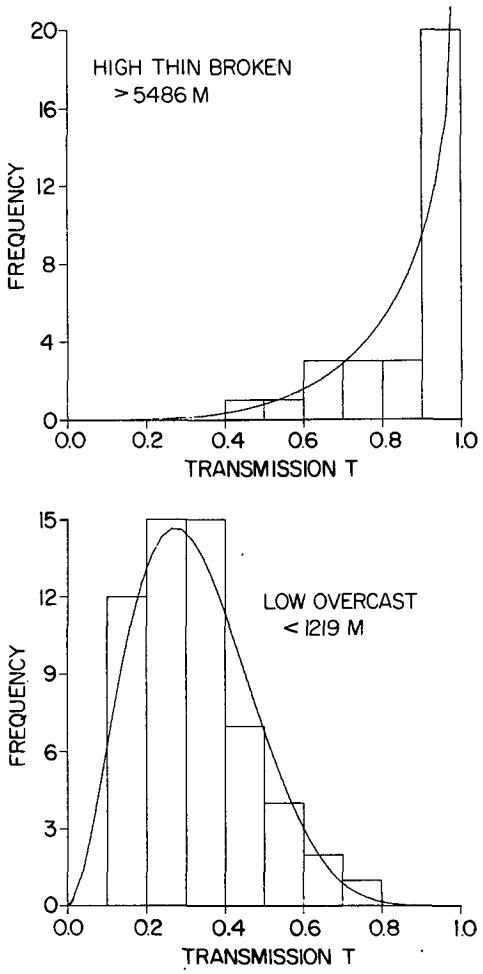

FIG. 1. Histogram and fitted Beta distribution of t_i for high thin broken and low overcast clouds.

rather than t_i means, the medians of the empirical distributions were selected as the t_i measure of central tendency to be used in (10) with the hourly cloud base heights and coverages. For SCT coverage, the median t_i for BKN layers was used.

To use the model (10), it was assumed: 1) that the radiative properties of the atmosphere do not change significantly when clouds are introduced, 2) that the hourly cloud observations are representative of the sky conditions during the time SR was computed, and 3) that the reported cloud layers are located between the observer (or pyranometer) and the sun.

To test the model, a random sample of 16% (five days if data were available for all days) was drawn from each month in 1980 for the following stations: Indianapolis, IN, Madison, WI, Nashville, TN, Omaha, NE, Columbia, MO, Seattle, WA, Los Angeles, CA, Phoenix, AZ, Lake Charles, LA, Miami, FL, and Sterling, VA. For West Lafayette, IN 120 days (33 percent) or ten days from each month in 1976 were randomly drawn. Using the reported cloud heights and coverages, the energy flux on a horizontal surface was computed every six minutes from sunrise to sunset and summed to give a daily total. Cloud observations made on the hour were assumed to hold from one half hour before to one half hour after the observation.

Scatter diagrams of daily SR, predicted versus measured, were plotted for each station, and the mean error, mean absolute error and rms error were computed for comparison. Regression equations were also computed to determine the slope and Y-intercept.

For a final test of the application of the model, solar radiation was estimated for the first and second order stations in Illinois, Indiana and Ohio for 1 and 12 April 1982, days with generally clear and variable cloud cover, respectively. The predicted SR was plotted and analyzed on daily charts and then compared with charts for the same days based on SR measurements from 19 special agricultural weather stations in the same three states.

3. Results and discussion

Daily totals of radiation computed from the cloud model for completely clear days were selected from the random samples for all stations tested. A plot of predicted versus observed SR for clear sky conditions at all stations is shown in Fig. 2. Excellent agreement was found for all levels of radiation. Although only the 1:1 line is shown on Fig. 2, the fitted regression of observed on estimated SR yielded an r^2 of 0.986, a slope of 0.96 (±0.01) and a y-intercept of 0.67 (±0.25) MJ m^{-2} day^{-1} (15.90 ly day^{-1}) indicating little bias in the model.

The mean error, mean absolute error and rms error were computed as follows:

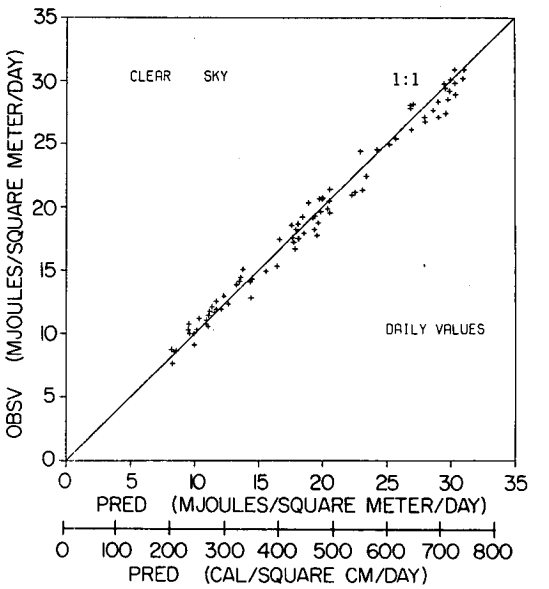

FIG. 2. Scatter diagram of predicted versus observed daily SR for clear sky conditions selected from the random samples for all stations.

$$\left.\begin{aligned} \text{mean error} &= \sum_{i=1}^{n} (\mathrm{SR_{pred}} - \mathrm{SR_{obsv}})/n \\ \text{mean absolute error} &= \sum_{i=1}^{n} |\mathrm{SR_{pred}} - \mathrm{SR_{obsv}}|/n \\ \text{rms error} &= \sum_{i=1}^{n} [(\mathrm{SR_{pred}} - \mathrm{SR_{obsv}})^2/n]^{1/2} \end{aligned}\right\}.$$

The mean error of 0.13 MJ m^{-2} day^{-1} (3.2 ly day^{-1}) shows little bias in the predicted SR for clear days. The mean absolute error was 0.72 MJ m^{-2} day^{-1} (17.22 ly day^{-1}) and the rms error (rmse) 0.86 MJ m^{-2} day^{-1} (20.60 ly day^{-1}). The predicted SR for clear sky conditions is generally within 5% of the observed values, common for most other solar radiation models.

The means and medians for the empirical distributions of the transmission coefficients (11) for each cloud height and coverage category are given in Table 1. The differences between BKN and OVC t_i for each layer are immediately apparent, especially for the low cloud heights. Below 1219 m, the median t_i for BKN layers is twice as large as that for OVC layers. As the cloud base height increases, the ratio of the BKN to OVC t_i medians decreases and approaches one for cloud layers greater than 5486 m. Almost all of the empirical distributions indicated some central tendency or peak, such as those shown in Fig. 1, with the t_i distributions for low clouds showing positive skew and those for high clouds, negative skew.

To estimate SR for cloudy conditions at any location, the t_i medians estimated for West Lafayette were used in Eq. (10) to obtain the estimated SR. For SCT coverage, the t_i for BKN coverage was used. Scatter diagrams of the observed with the predicted SR are shown in Fig. 3 for the indicated locations arranged as much as possible in geographical order. A 1:1 line was drawn in each diagram to show the ideal response. Regressions of observed on predicted daily SR were calculated for each station. The r^2, slope and intercept, with the corresponding standard errors, are shown in Table 2. Almost all of the slopes (b_1) were within one standard deviation of 1.0. The largest intercept was for Miami with a value of 1.68 MJ m^{-2} day^{-1}. The remaining intercepts were all close to zero indicating little bias in predicting daily SR. The r^2 for all stations were greater than 0.90 except for Miami which yielded an r^2 of 0.77.

The mean errors, mean absolute errors, and rms errors are shown in Table 3. The mean absolute errors ranged from 1.05 MJ m^{-2} day^{-1} (25.02 ly day^{-1}) at Los Angeles to 1.80 MJ m^{-2} day^{-1} at Miami. The mean absolute error for all stations combined was 1.28 MJ m^{-2} day^{-1} well within 10% of the observed SR with a mean daily SR of 14.64 MJ m^{-2} day^{-1}. The rms error followed the same pattern, ranging from 1.31 MJ m^{-2} day^{-1} at Los Angeles to 2.32 MJ m^{-2} day^{-1} for Miami. Mean errors ranged from −0.65 MJ m^{-2} day^{-1} at Miami to 0.48 MJ m^{-2} day^{-1} at Lake Charles. For all stations the mean error was −0.12 MJ m^{-2} day^{-1} and the rms error 1.69 MJ m^{-2} day^{-1}. The rms errors are about half of those obtained by Atwater and Ball (1981), whose lowest rms error was 3.21 MJ m^{-2} day^{-1}. The results are also as good as those obtained with GOES satellite measurements by Gautier *et al.* (1980), who estimated SR generally within 10% of the measured values for three stations in Canada. The model in this paper was subjected to more rigorous testing because observational sites were selected from diverse climates in the United States.

The SR predictions for each station were also investigated to determine if there was a correlation between errors and seasons. The mean error, mean absolute error and rms error were calculated and compared for the periods January–March, April–June, July–September and October–December as shown in Table 4. The largest mean absolute errors occurred during the periods April–June or July–September for all stations except Nashville, where the largest error occurred in the period from January–March. For the other eleven stations the mean absolute errors ranged from 1.03 MJ m^{-2} day^{-1} at Los Angeles to 2.82 MJ m^{-2} day^{-1} at Miami for the combined periods from April–September. The rms error followed the same trend with slightly higher values. The smallest mean absolute errors occurred during the period October–December for the majority of the stations with a range from 0.54 to 1.50 MJ m^{-2} day^{-1}. When a percentage error was computed by dividing the mean absolute error by the mean daily SR, however, there appeared to be no correlation between seasons and mean percentage error. The computed percentage errors for all stations were about 10 ± 2%.

TABLE 1. Mean and median t_i for the empirical distributions of cloud transmission coefficients and ratio of median t_i for broken (BKN) to overcast (OVC) cloud layers, for indicated heights and coverages.

Height (m)	Coverage	Median t_i	Mean t_i	t_{BKN}/t_{OVC}
<1219	OVC	0.31	0.32	
<1219	BKN	0.63	0.64	2.03
1219–3048	OVC	0.41	0.43	
1219–3048	BKN	0.53	0.55	1.29
3048–5486	OVC	0.46	0.47	
3048–5486	BKN	0.52	0.63	1.13
>5486	OVC	0.67	0.67	
>5486	BKN	0.66	0.72	0.99
>5486 thin	OVC	0.87	0.83	
>5486 thin	BKN	0.95	0.86	1.10

Some of the differences between predicted and observed daily SR could be attributed to errors in estimating clear sky transmission. The expression for aerosol attenuation (8) assumes an average aerosol opacity throughout the year. Inaccuracies in this assumption, however, are not considered to be a large portion of the error between predicted and observed values for the stations used in this investigation because the model proved to be effective for clear sky transmission.

Another possible source of error involves the use of the surface dewpoint to estimate precipitable water rather than the more accurate method of computing precipitable water from radiosonde data. Since the mean daily dewpoint was used, changes in precipitable water throughout the day may not be reflected in the equation for water vapor transmission. Although Atwater and Ball (1976) found annual average differences of less than 1% between SR estimates using the radiosonde data and those using the surface dewpoint to obtain the precipitable water, the error could be larger on any individual day.

Undoubtedly, the largest contribution to the total error between predicted and observed daily SR originated from use of the median t_i (Table 1, Fig. 1). The median t_i may not reflect the proper transmissivity of the clouds, because cloud thickness, liquid water content and cloud drop size distribution may change rapidly with time. Since the cloud transmission coefficients were derived empirically with data from West Lafayette, and the zenith angle dependence of finite clouds was not included (Davis *et al.*, 1979), the results may not apply to all locations. Errors may originate from cloud attenuation within cer-

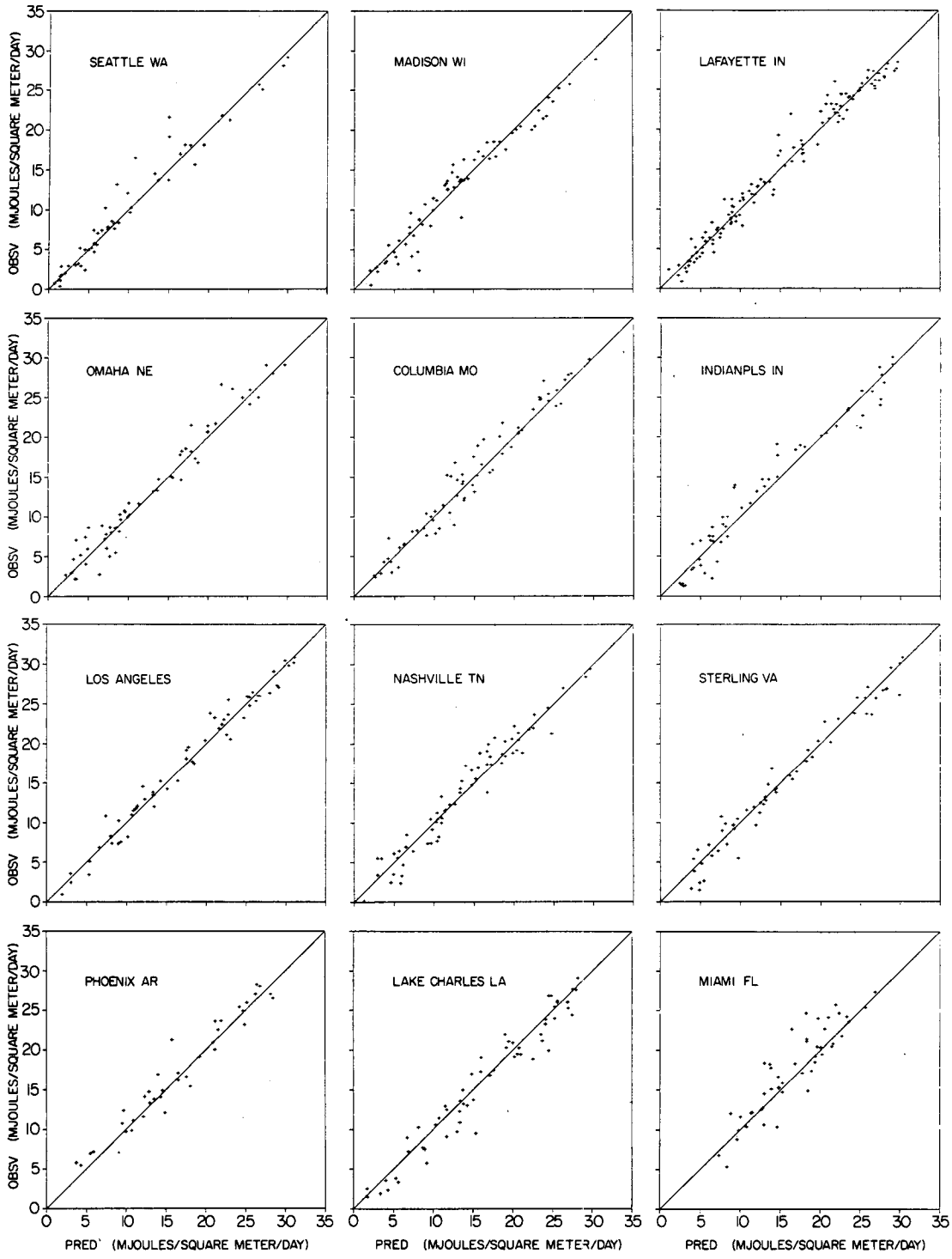

FIG. 3. Scatter diagrams of predicted versus observed daily SR for randomly selected days for indicated stations.

tain spectral bands. With multiple cloud layers a broad band cloud transmission coefficient may not account for the selective absorption and scattering by each layer. Cloud observations made on the hour also may not be representative of the sky conditions during the hour for which the insolation was estimated. Clouds reported may not always be between the sun and the observer (or pyranometer). Errors of this type

TABLE 2. Coefficient of determination (r^2), slope (b_1), intercept (b_0) and standard errors (s_{b1}, s_{b0}) for the regression of observed on predicted daily solar radiation (SR), for indicated station and random sample size (n).

Station	r^2	b_1	s_{b1}	b_0	s_{b0}	n
Los Angeles, CA	0.975	0.988	± 0.02	0.25	± 0.40	59
Sterling, VA	0.966	0.988	± 0.02	−0.09	± 0.43	58
Phoenix, AZ	0.947	0.947	± 0.04	1.41	± 0.68	38
Miami, FL	0.777	0.962	± 0.07	1.68	± 1.28	49
Lake Charles, LA	0.947	0.998	± 0.03	−0.43	± 0.58	59
Seattle, WA	0.950	0.976	± 0.03	0.60	± 0.40	53
West Lafayette, IN	0.973	0.984	± 0.02	0.40	± 0.26	120
Indianapolis, IN	0.954	0.984	± 0.03	0.39	± 0.47	57
Omaha, NE	0.957	1.009	± 0.03	0.29	± 0.43	57
Madison, WI	0.943	0.964	± 0.03	0.27	± 0.44	64
Columbia, MO	0.955	1.027	± 0.03	−0.01	± 0.45	66
Nashville, TN	0.940	1.016	± 0.03	0.03	± 0.49	68
Clear days for all stations	0.986	0.960	± 0.01	0.67	± 0.25	85

may be especially frequent at low sun angles. The climatology of cloud type differs spatially as reflected in the occurrence of the lowest error at Los Angeles, CA and the greatest at Miami, FL and Lake Charles, LA. Yet, with all these possible sources of error, the excellent results indicate that the errors may be offsetting when averaged over the day.

4. Application of the model

The usefulness of the model is illustrated with the predicted and measured daily SR charts for 1 and 12 April 1982 in Figs. 4 and 5, respectively for the three-state region of Illinois, Indiana and Ohio. On 1 April there was little cloudiness over the region and little SR gradient. Solar radiation was generally above

TABLE 3. Mean error, mean absolute error, and root mean square error (rmse) for predicted daily solar radiation (SR) for all stations tested. Units are MJ m^{-2} day^{-1}, with ly day^{-1} in parentheses.

Station	Mean error	Mean absolute error	rmse
Los Angeles, CA	−0.05 (−1.19)	1.05 (25.02)	1.31 (31.40)
Sterling, VA	0.28 (6.69)	1.18 (28.17)	1.53 (36.70)
Phoenix, AZ	−0.53 (−12.58)	1.29 (30.89)	1.61 (38.40)
Miami, FL	−0.65 (−15.51)	1.80 (43.00)	2.32 (55.60)
Lake Charles, LA	0.48 (11.36)	1.49 (35.66)	1.84 (44.00)
Seattle, WA	−0.35 (−8.42)	1.12 (26.83)	1.78 (42.50)
West Lafayette, IN	−0.38 (−9.15)	1.06 (25.33)	1.40 (33.50)
Indianapolis, IN	0.07 (1.81)	1.34 (32.13)	1.92 (45.90)
Omaha, NE	−0.41 (−9.75)	1.25 (29.87)	1.64 (39.10)
Madison, WI	0.19 (4.47)	1.27 (30.35)	1.68 (40.20)
Columbia, MO	−0.37 (−8.89)	1.27 (30.36)	1.63 (39.00)
Nashville, TN	−0.19 (−4.70)	1.30 (31.07)	1.66 (39.70)
All stations	−0.12 (−2.81)	1.28 (30.71)	1.69 (40.50)
Clear days for all stations	0.14 (3.24)	0.72 (17.21)	0.86 (20.60)

TABLE 4. Mean error, mean absolute error and root mean square error (rmse) for predicted solar radiation (SR) for indicated station, seasonal period, and random sample size (n). Units as in Table 3.

Station	Mean error	Mean absolute error	rmse	n
West Lafayette, IN				
January–March	−0.94 (−9.63)	0.87 (20.97)	1.00 (24.0)	30
April–June	−0.13 (−3.07)	1.35 (32.20)	1.79 (42.7)	30
July–September	0.04 (0.97)	1.25 (29.97)	1.66 (39.7)	30
October–December	−0.15 (−3.47)	0.77 (18.47)	1.00 (24.1)	30
Indianapolis, IN				
January–March	0.69 (16.57)	1.34 (32.14)	1.44 (34.3)	22
April–June	0.10 (−2.45)	1.61 (38.65)	2.26 (54.0)	20
July–December	0.48 (11.47)	1.52 (36.27)	1.97 (47.0)	15
Los Angeles, CA				
January–March	0.12 (2.80)	1.39 (33.33)	1.68 (40.2)	15
April–June	−0.18 (−4.20)	1.05 (25.00)	1.43 (34.2)	15
July–September	0.09 (2.13)	1.04 (24.80)	1.24 (29.7)	15
October–December	−0.21 (−4.93)	0.66 (15.73)	0.81 (19.4)	15
Miami, FL				
January–March	−0.29 (−6.93)	0.99 (23.70)	1.41 (33.7)	14
April–June	−0.85 (−20.27)	2.81 (67.20)	3.25 (77.7)	15
July–September	−0.58 (−13.80)	2.67 (64.20)	2.99 (71.5)	15
October–December	−0.38 (−9.00)	0.86 (20.60)	1.12 (26.7)	05
Omaha, NE				
January–March	−0.83 (−19.78)	1.56 (37.33)	1.75 (41.9)	18
April–June	−0.18 (−4.27)	1.95 (46.64)	2.46 (58.8)	11
July–September	−0.07 (−1.60)	1.20 (28.74)	1.59 (37.9)	10
October–December	−0.32 (−7.67)	0.57 (13.56)	0.73 (17.4)	18
Madison, WI				
January–March	−0.58 (−13.78)	1.28 (30.67)	1.75 (42.0)	18
April–June	0.32 (7.76)	1.43 (34.21)	1.76 (42.1)	17
July–September	0.55 (13.06)	1.42 (34.00)	1.80 (43.1)	17
October–December	0.63 (15.00)	0.84 (20.17)	0.88 (21.0)	12
Columbia, MO				
January–March	−0.53 (−12.60)	0.98 (23.40)	1.26 (30.2)	15
April–June	−0.80 (−19.06)	2.00 (47.81)	2.30 (55.0)	16
July–September	−0.92 (−22.00)	1.68 (40.17)	1.76 (42.0)	12
October–December	0.31 (7.35)	0.75 (17.87)	0.98 (22.4)	23
Nashville, TN				
January–March	0.45 (10.72)	1.57 (37.61)	1.82 (43.6)	18
April–June	−0.02 (−0.50)	1.35 (32.28)	1.78 (42.6)	18
July–September	−0.97 (−23.20)	1.53 (36.67)	1.72 (41.1)	15
October–December	−0.18 (−4.24)	0.78 (18.53)	0.97 (23.2)	17
Sterling, VA				
January–March	0.65 (15.60)	1.37 (32.80)	1.80 (43.2)	15
April–June	0.02 (−0.40)	1.21 (28.93)	1.63 (38.9)	15
July–September	0.69 (16.40)	1.42 (33.87)	1.58 (37.7)	15
October–December	0.28 (−6.62)	0.64 (15.38)	0.74 (17.7)	13
Seattle, WA				
January–March	0.10 (−2.40)	0.84 (20.13)	1.27 (30.3)	15
April–June	0.53 (−12.56)	2.70 (64.56)	3.21 (76.7)	09
July–September	0.12 (−2.79)	1.03 (24.64)	1.54 (36.9)	14
October–December	0.03 (0.80)	0.54 (12.93)	0.69 (16.4)	15
Lake Charles, LA				
January–March	0.47 (11.21)	1.17 (28.07)	1.43 (34.1)	14
April–June	0.92 (22.00)	2.00 (47.73)	2.41 (57.7)	15
July–September	0.40 (−9.67)	1.51 (36.07)	1.89 (45.1)	15
October–December	0.96 (22.87)	1.29 (30.75)	1.19 (28.5)	16
Phoenix, AZ				
January–March	0.64 (15.35)	1.11 (26.57)	1.27 (30.3)	23
April–June	0.80 (−19.20)	2.41 (57.60)	2.71 (64.8)	05
July–September	0.10 (−2.50)	1.10 (26.30)	1.36 (32.6)	10

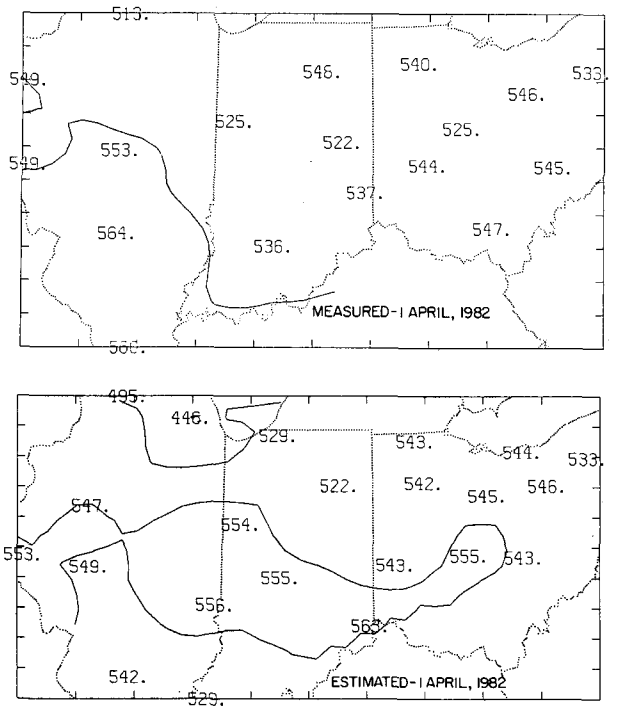

FIG. 4. Charts of predicted (lower) and measured (upper) daily SR (ly day^{-1}) for three-state region of Illinois, Indiana and Ohio on 1 April 1982.

20.92 MJ m^{-2} day^{-1} (500 ly day^{-1}) throughout the region. On 12 April, the predicted solar radiation ranged from a low of 9.5 MJ (227 ly) at South Bend, IN, to a high of 24.18 MJ m^{-2} at Mount Vernon, IL. Although the predicted and observed patterns are similar, differences in the analysis are produced by the different station networks. The SR analyses for the pooled observed and predicted stations for 1 and 12 April 1982 are shown in Fig. 6. Should our knowledge of the current use of SR data warrant such an analysis, the model could be used with the NWS/AFOS network data in real time to prepare charts such as those shown for the predicted SR (first and second order network) in Figs. 4 and 5 and, with arrangements for including the special agricultural meteorological observations, Fig. 6 for the entire U.S. Such an analysis provides a better means of quality control for the SR measurements than is presently possible with the sparse SOLMET network. For example, in testing the model with 1980 SR data from West Lafayette, it became apparent that the pyranometer output was only 80% of what it should be. The situation was corrected along with the erroneous data. The excellent agreement of the predicted with the measured SR, shown in Fig. 3, attests to satisfactory calibration of the SR data published for the SOLMET network in 1980.

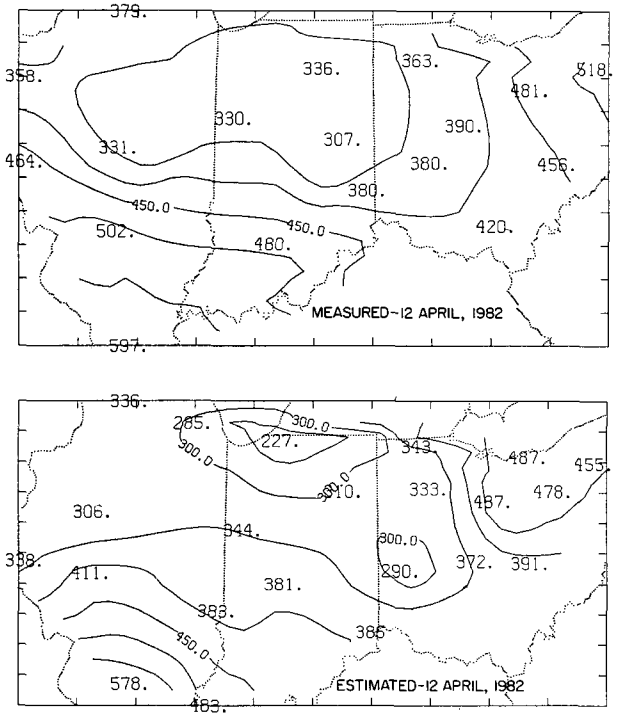

FIG. 5. Charts of predicted (lower) and measured (upper) daily SR (ly day^{-1}) for three-state region of Illinois, Indiana and Ohio on 12 April 1982.

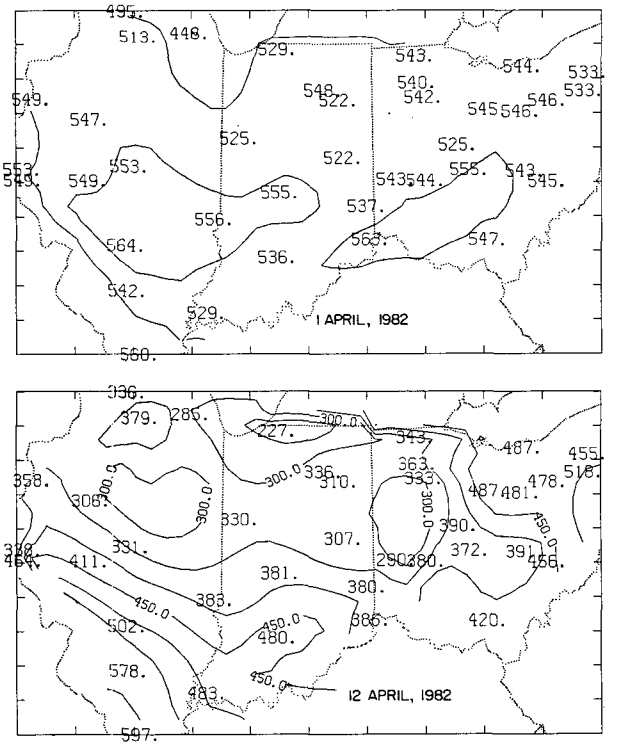

FIG. 6. Charts of pooled estimates and measurements of daily SR for 1 and 12 April 1982.

5. Conclusions

Cloud height and coverage, together with empirical expressions for clear sky transmission were shown to be effective in estimating daily SR to within 10% of the measured values for most regions in the United States. Mean absolute errors were on the order of 1.4 MJ m^{-2} day^{-1} with the largest errors occurring for stations along the Gulf of Mexico. To improve the accuracy of the model in these regions different cloud transmission coefficients could be derived and tested. Treating atmospheric absorption and scattering within different spectral bands, rather than as a percentage transmission, would more closely simulate the real atmosphere and possibly improve the results.

The model presented can be used effectively to enhance the existing sparse SR network and can also provide a means of quality control for SR measurements. With the network of first and second order stations, the spatial distribution of daily SR can be assessed for applications in crop modeling and design of solar energy systems.

Acknowledgments. The solar radiation measurements in Ohio are provided daily to the NWS-Purdue Midwest Agricultural Weather Service Center (MAWSC) by Dr. R. Bruce Curry of the Ohio Agricultural Research and Development Center (OARDC), at Wooster, OH, and Dr. John Klink, Miami University, Oxford, OH. The Illinois pyranometer measurements were furnished by Mr. Keith Hendrie of the Illinois State Water Survey, Urbana. The graphics routine used for the production of the daily SR charts was furnished by Dr. David Smith of the Geosciences Dept. Purdue University. The authors also thank the JCAM reviewers for their constructive comments on this paper.

REFERENCES

Atwater, M. A., and J. T. Ball, 1981: A surface solar radiation model for cloudy atmospheres. *Mon. Wea. Rev.*, **109,** 878–888.

——, and ——, 1978: Intraregional variations of solar radiation in the eastern United States. *J. Appl. Meteor.*, **17,** 1116–1125.

——, and ——, 1976: Comparisons of radiation computations using observed and estimated precipitable water. *J. Appl. Meteor.*, **15,** 1319–1320.

——, and P. S. Brown, Jr., 1974: Numerical computation of the latitudinal variations of solar radiation for an atmosphere of varying opacity. *J. Appl. Meteor.*, **13,** 289–297.

Bolsenga, S. J., 1965: The relationship between total atmospheric water vapor and surface dewpoint on a mean daily and hourly basis. *J. Appl. Meteor.*, **4,** 430–432.

Brakke, T. W., and E. T. Kanemasu, 1981: Insolation estimation from satellite measurements of reflected radiation. *Remote Sens. Environ.*, **11,** 157–167.

Davies, J. A., W. Schertzer and M. Nunez, 1975: Estimating global solar radiation. *Bound.-Layer Meteor.*, **9,** 33–51.

Davis, J. M., S. K. Cox and T. B. McKee, 1979: Total shortwave characteristics of absorbing finite clouds. *J. Atmos. Sci.*, **36,** 508–518.

Gautier, C., G. Diak and S. Masse, 1980: A simple physical model to estimate incident solar radiation at the surface from GOES satellite data. *J. Appl. Meteor.*, **19,** 105–1112.

Haurwitz, G., 1948: Insolation in relations to cloud type. *J. Meteor.*, **5,** 110–113.

Houghton, H. G., 1954: On the annual heat balance of the Northern Hemisphere. *J. Meteor.*, **11,** 1–9.

Kondratyev, K., 1969: *Radiation in the Atmosphere,* Academic Press, 912 pp.

Manabe, S., and R. S. Strickler, 1964: Thermal equilibrium of the atmosphere with a convective adjustment. *J. Atmos. Sci.*, **21,** 361–385.

McDonald, J. E., 1960: Direct absorption of solar radiation by atmospheric water vapor. *J. Meteor.*, **17,** 319–328.

Meyers, T. P., R. F. Dale and J. G. Wright, 1982: Estimating solar radiation on a horizontal surface. *Proc. Indiana Acad. Sci.*, **90,** 563–571.

Reitan, C. H., 1963: Surface dewpoint and water vapor aloft. *J. Appl. Meteor.*, **2,** 776–779.

Smith, W. L., 1966: Note on the relationship between total precipitable water and surface dewpoint. *J. Appl. Meteor.*, **5,** 726–727.

Suckling, P. W., and J. E. Hay, 1977: A cloud layer sunshine model for estimating direct, diffuse and total solar radiation. *Atmosphere,* **15,** 194–207.

Walraven, R., 1978: Calculating the position of the sun. *Sol. Energy,* **20,** 393.